

Targeted Approach to Distinguish and Determine Absolute Levels of GDF8 and GDF11 in Mouse Serum

Luca Campanini, Laxmikanth Kollipara, Gianfranco Sinagra, Francesco S. Loffredo, Albert Sickmann, and Olga Shevchuk*

Growth differentiation factor 11 (GDF11) is a TGF- β superfamily circulating factor that regulates cardiomyocyte size in rodents, sharing 90% amino acid sequence identity in the active domains with myostatin (GDF8)—the major determinant of skeletal muscle mass. Conflicting data on age-related changes in circulating levels have been reported mainly due to the lack of specific detection methods. More recently, liquid chromatography tandem mass spectrometry (LC-MS/MS) based assay showed that the circulating levels of GDF11 do not change significantly throughout human lifespan, but GDF8 levels decrease with aging in men. Here a novel detection method is demonstrated based on parallel reaction monitoring LC-MS/MS assay combined with immunoprecipitation to reliably distinguish GDF11 and GDF8 as well as determine their endogenous levels in mouse serum. The data indicate that both GDF11 and GDF8 circulating levels significantly decline with aging in female mice.

1. Introduction

Growth differentiation factor 11 (GDF11) is a TGF- β superfamily circulating factor that regulates cardiomyocyte size in rodents.^[1,2] GDF11 shares 90% amino acid sequence identity in the active domains with myostatin (GDF8), the major determinant of skeletal muscle mass. After processing by furin-like proteases, both GDF11 and GDF8 are secreted as an inactive latent complex that is activated by cleavage of the prodomain by BMP-1/tolloid family metalloproteases and release of the active dimer GDF8 and GDF11 activate the SMAD2/3 pathway binding activin type II and type I (ALK4/5/7) receptors. Nevertheless, additional pathways, including mitogen-activated protein kinase signaling, have

been reported.^[3] Although highly similar, a distinctive expression pattern and critical differences in active domains that affect the interaction with receptors and inhibitors confer GDF11 and GDF8 to a distinct functional role, different potency, and cell-type specificity.^[3,4]

The high homology between GDF11 and GDF8 has also contributed to generate contrasting data on age-related changes in circulating levels, mainly because of the detection methods. Indeed, aptamers, western blot, and ELISA were not enough specific to discriminate these two ligands.^[2] Initial findings on circulating levels of GDF11, using aptamer and antibody-based quantification that do not accurately distinguish GDF11 from GDF8, have indeed shown an age-dependent decline in mice^[1] or potentially an increase in rats and humans.^[5] When considering GDF11 and GDF8 together, an age-dependent decline in serum GDF11/8 levels in different mammalian species was observed.^[2] A more specific approach using liquid chromatography tandem mass spectrometry (LC-MS/MS) based assay determined that while GDF11 circulating levels do not significantly change throughout human lifespan,^[6,7] GDF8 levels decrease with aging in men.^[6]


Given the potential specific role of GDF11 and GDF8 in aging and in regulating important biological processes, a specific and reliable method to determine their levels in biological samples is required. Therefore, we developed a parallel reaction monitoring (PRM) LC-MS/MS-based assay combined with immunoprecipitation (IP) for GDF11/8 enrichment. The method reliably detects and distinguishes GDF8 and GDF11. Using stable isotope-labeled (SIL) peptides, we have determined the endoge-

Dr. L. Campanini, Prof. F. S. Loffredo
Molecular Cardiology
International Centre for Genetic Engineering and Biotechnology (ICGEB)
Padriciano, 99 - 34149, Trieste Trieste, Italy

Prof. G. Sinagra
Division of Cardiology
Cardiovascular Department
Azienda Sanitaria Universitaria Integrata di Trieste (ASUITS)
Via Slataper, 9 - 34134, Trieste, Trieste, Italy

Dr. L. Kollipara, Prof. A. Sickmann, Dr. O. Shevchuk
Leibniz Institut für Analytische Wissenschaften—ISAS—e.V.
Bunsen-Kirchhoff-Straße 11 | 44139 Dortmund, Germany, Dortmund,
Germany
E-mail: olga.shevchuk@isas.de

Prof. F. S. Loffredo
Division of Cardiology
Department of Translational Medical Sciences
University of Campania
Via Leonardo Bianchi - 80131, Napoli Napoli, Italy

 The ORCID identification number(s) for the author(s) of this article can be found under <https://doi.org/10.1002/pmic.201900104>

© 2020 The Authors. *Proteomics* published by WILEY-VCH Verlag GmbH & Co. KGaA, Weinheim. This is an open access article under the terms of the Creative Commons Attribution-NonCommercial-NoDerivs License, which permits use and distribution in any medium, provided the original work is properly cited, the use is non-commercial and no modifications or adaptations are made.

DOI: 10.1002/pmic.201900104

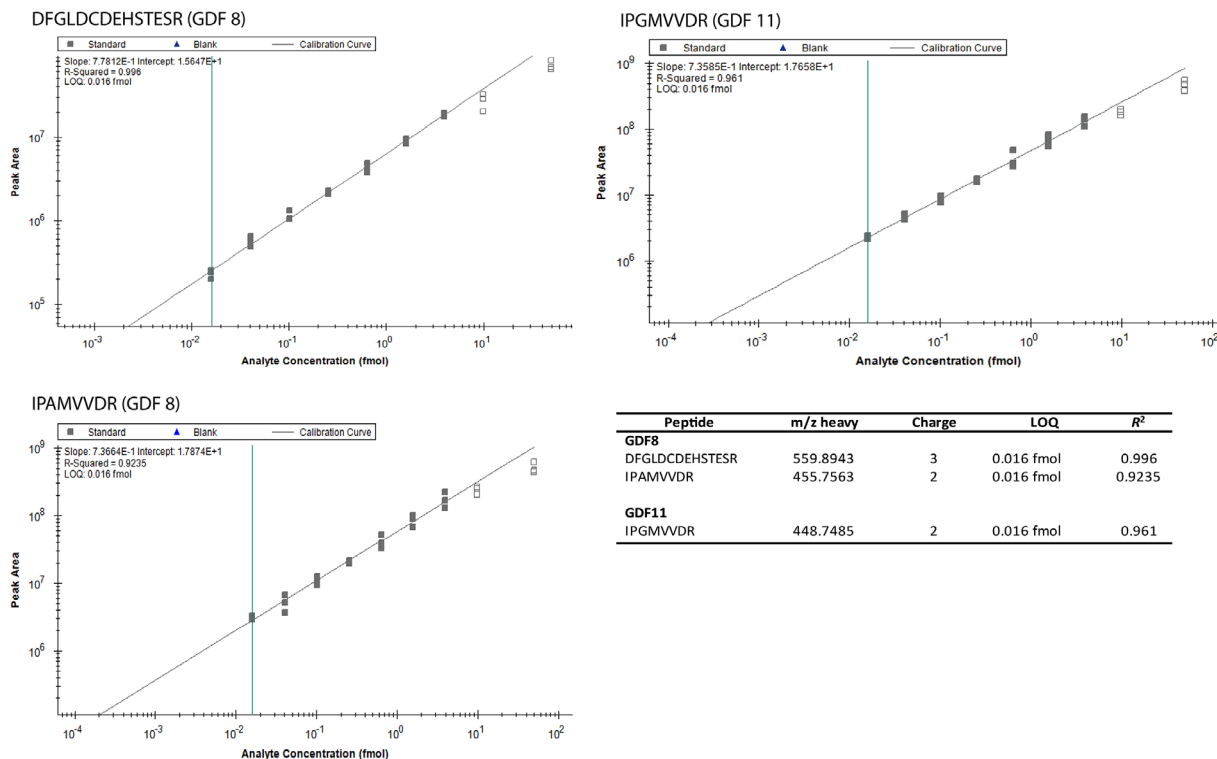


Figure 1. The calibration curves were generated using a WT serum matrix. An equimolar mixture of SIL peptides was added before injection at an increasing amount from 16 amol to 50 fmol. The horizontal axis represents the quantity of SIL peptide injected; the vertical axis represents the sum area of fragment ions gained by PRM. Data are represented as the mean of three technical replicates (STDEV) to calculate coefficients of variation (CVs, %) and calibration curve value (R^2). Horizontal green lines represent LLOQ.

nous concentrations of both proteins in the serum of young and aging mice and showed that both factors decline during aging.

2. Assay Development

The assay method was developed using Skyline software Skyline 64-bit version 4.2.0.19072.^[8] The peptides for detection of GDF8 and GDF11 were selected based on i) their uniqueness, ii) fully tryptic with no missed cleavage sites, and iii) a length of 8–25 amino acid residues to ensure reliable protein quantification (see Supporting Information). Initially, five and four proteotypic peptides of GDF11 and GDF8, respectively, were selected to establish PRM based targeted-MS/MS assay using a WT mouse serum tryptic digest (see Supporting Information for serum digest preparation) with their respective spiked-in SIL versions using Orbitrap Lumos. However, detection of endogenous GDF11 peptides could not be achieved with conventional PRM MS settings on this instrument. Therefore, as shown recently by Nguyen CDL et al., the sensitivity of targeted-MS technologies can be enhanced for detecting low-abundant proteins/peptides by systematically optimizing the key MS parameters, such as resolution (R) and ion injection/fill times.^[9] Employing their strategy, we empirically and iteratively performed several PRM measurements focusing on different combinations of MS settings (see Supporting Information for details). However, even at R 500 K and 1024 ms fill time (Figure S1, Supporting Information), it was not sufficiently efficient to detect low abundant endoge-

nous GDF11 peptides, whereas the peptides belonging to GDF8 were readily detected in the WT serum digest under these conditions. It was indeed a challenging task to detect the endogenous peptides of GDF11 and GDF8 simultaneously in a single targeted-MS assay and from direct serum digest. Therefore, for enrichment of the desired analytes, we decided to introduce an antibody-based approach prior to PRM LC-MS/MS analysis.^[6,10] Biotinylated antibodies were tested a side of not-biotinylated ones and no loss of binding activity was observed after biotinylation. The efficiency of IP was examined for each antibody individually and verified by western blot (Figure S2, Supporting Information).

For the final targeted assay, three heavy/light pair peptides (six precursors) of both GDF11 (IPGMVVDR) and GDF8 (IPAMVVDR, DFGLDCDEHSTESR), which were free from interference and suitable for generating calibration curves and quantitation of endogenous peptides were selected. Targeted PRM analyses with R 120 K, 256 ms fill time MS settings were performed for peptide samples after IP (see Supporting Information for IP sample preparation).

3. Targeted (PRM)–LC-MS/MS Analysis

Unless otherwise stated, all samples (i.e., calibration curves and IP eluates) were analyzed using an Ultimate 3000 nano RSLC system (UV absorbance at 214 nm) coupled to Orbitrap Lumos (both Thermo Scientific). Additionally, to check for any carry-over, blank measurements were performed in between calibra-

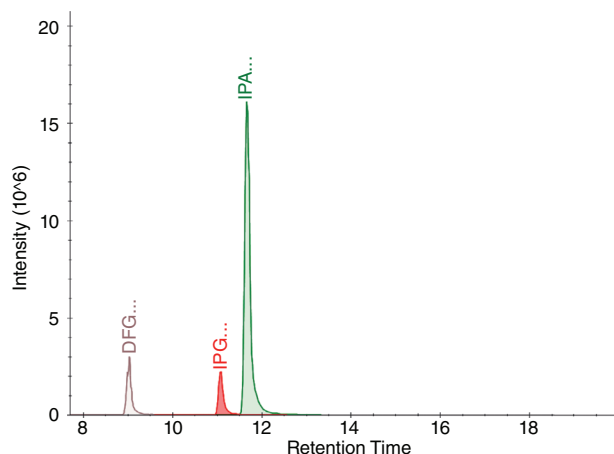


Figure 2. Distinguishing of two closely related peptides IPAMVVDR (GDF8) and IPGMVVDR (GDF11). IPAMVVDR (GDF8) was resolved from IPGMVVDR (GDF11) with respect to retention time and based on unique precursor m/z and fragmentation ions pattern.

tion curve samples as well as at the beginning and the end of IP samples using the same LC-MS/MS settings. A fraction (40% of total eluate) of each IP sample was analyzed in a randomized order to account for any systematic errors. Briefly, peptide samples were preconcentrated on a $100 \mu\text{m} \times 2 \text{ cm}$ C18 trapping column for 5 min using 0.1% TFA with a flow rate of $20 \mu\text{L min}^{-1}$ followed by separation on $75 \mu\text{m} \times 50 \text{ cm}$ C18 analytical column (both Acclaim Pepmap nanoViper, Thermo Scientific) using a 30 min gradient ranging from 5–25% B (84% ACN in 0.1% FA) at a flow rate of 250 nL min^{-1} .

The Orbitrap Lumos was operated in PRM mode using the following settings: MS/MS scans were acquired in the Orbitrap at a resolution of 120 000 with an automatic gain control target value of 1×10^5 ions and a maximum injection time of 246 ms. Precursor ions were isolated using 0.4 m/z width, and fragmentation was performed in the HCD cell with a normalized collision energy of 32% as triggered by the provided inclusion list. Thus generated raw MS/MS data were imported into Skyline for visualization, manual validation, mass error (Δ ppm), and assignment of retention time boundaries, for example, 3 min as predicted by Skyline.

4. Generation of Calibration Curves with SIL Peptides and Final PRM Measurements

Multipoint response calibration curves were generated using a mixture of SIL peptides of both GDF11 (IPGMVVDR) and GDF8 (IPAMVVDR, DFGLCDCEHSTESR) spiked in a matrix consisting of 200 ng of digested mouse serum. A stock solution of SIL peptides was prepared and serially diluted such that the final amount of each SIL peptide per injection was 50, 10, 4, 1.6, 0.64, 0.256, 0.102, 0.041, and 0.016 fmol by keeping the background matrix constant, that is, 200 ng. The samples were analyzed from the lowest to the highest amount in three technical replicates. Calibration curves were constructed by plotting the peak area of the SIL peptide versus the analyte amount. The lowest limit of quantification (LLOQ) for the particular SIL peptide was defined as the lowest concentrations of the dilution series, which had less

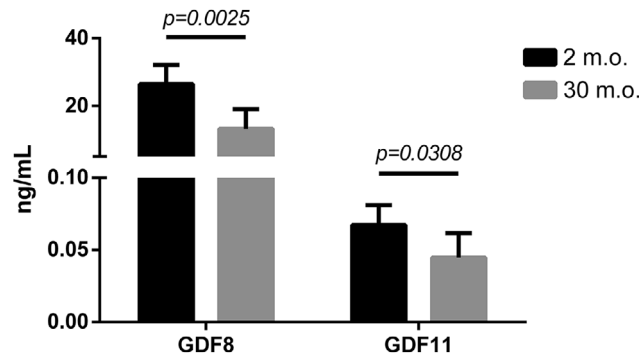


Figure 3. The concentration of GDF8 and GDF11 in serum (ng mL^{-1} of starting material) of young and old mice determined by targeted assay. Both GDF8 and GDF11 significantly decline with aging. $**p = 0.0025$, $*p = 0.0308$. Data are shown as mean \pm SD.

than 20% of standard deviation within three replicates (Figure 1; Tables S1,S2, Supporting Information).

Furthermore, peptide IPGMVVDR (GDF11) was clearly resolved from IPAMVVDR (GDF8) with respect to its i) unique precursor m/z , ii) fragment ions pattern, and iii) retention time (Figure 2; Table S3, Supporting Information). Finally, based on the results from calibration curves (i.e., LLOQ) and roughly estimated levels of GDF11 and GDF8 obtained from our optimization experiments, we spiked-in 2 fmol of each SIL peptide to all IP eluates before PRM LC-MS/MS analysis.

5. Data Evaluation and Statistics

PRM experiments were performed using a scheduled (3-min window) inclusion list generated in Skyline.^[8] The inclusion list consisted of m/z of each precursor along with collision energy and corresponding retention times obtained by an unscheduled run. The list of precursors, their product ions, and corresponding m/z are in Table S1, Supporting Information. MS raw files were imported to Skyline, and acquired data were reviewed and integrated manually. Identification and quantification of the endogenous peptides were based on the following criteria: i) integration of fragment ions with narrow mass tolerances (≤ 5 ppm), ii) ≥ 4 peptide specific fragment ions, iii), dot product (dotp) value^[11] ≥ 0.93 , and iv) without any background interference. The quantification was performed using the sum of peak areas obtained for each peptide fragment ion. The raw data are available at ProteomeXchange (PXD008395) and the entire PRM data set can be viewed as a Skyline document in Panorama Public via the following link: <https://panoramaweb.org/BnW2U9.url>.^[8,12]

For each biological replicate/condition, we took the average heavy to light (H/L) ratios of two peptides of GDF8, whereas for GDF11, the H/L ratio of the single peptide was considered. These values were subsequently used to calculate endogenous values and standard deviations. For statistics, unpaired two-tailed Student's t -test was applied for comparing two groups of animals by using GraphPad software (Prism, La Jolla, CA, USA).

Received: October 18, 2019

Revised: January 31, 2020

Published online: May 13, 2020

6. Circulating GDF8 and GDF11 Decline with Aging in Mice

To our knowledge, no study has investigated serum levels of GDF11 and GDF8 in mice using a specific quantitative nanoLC-high resolution MS approach. Therefore, an optimized PRM assay combined with IP was applied in a pilot study aiming to compare serum levels of GDF11 and GDF8 between young (2 months, $n = 6$) and old (30 months, $n = 6$) female mice. IP followed by proteolysis of GDF11/8 were highly reproducible (Figure S3, Supporting Information), and subsequent PRM LC-MS/MS assay data were used for quantification of both proteins (Tables S4,S5, Supporting Information). We observed a significant decrease of both GDF8 (26.489 ± 5.621 vs 13.190 ± 5.860 ng mL⁻¹, $p = 0.0025$) and GDF11 (0.0673 ± 0.0138 vs 0.0446 ± 0.0171 ng mL⁻¹, $p = 0.0308$) in the serum of 30-month old female C57Bl/6 mice compared to young mice (Figure 3). Interestingly, circulating GDF11 in mice is ten times less than in humans and more than two orders of magnitude lower than circulating GDF8.^[6,7] The biological relevance of these findings require further investigations, including the role of gender and pathological conditions in contributing to changes in circulating levels.

Supporting Information

Supporting Information is available from the Wiley Online Library or from the author.

Acknowledgements

L.C., F.L., and G.S. acknowledge the support by the ICGEB core funding, Casali Foundation (Trieste), and "CardioRiGen" from the Italian Ministry of Health. L.K., A.S., and O.S. acknowledge the support by the Ministerium für Kultur und Wissenschaft des Landes Nordrhein-Westfalen, the Regierende Bürgermeister von Berlin–inkl. Wissenschaft und Forschung, and the Bundesministerium für Bildung und Forschung.

Conflict of Interest

The authors declare no conflict of interest.

Keywords

aging, GDF11, immunoprecipitation, myostatin/GDF8, serum, targeted-quantitative proteomics

- [1] F. S. Loffredo, M. L. Steinhauser, S. M. Jay, J. Gannon, J. R. Pancoast, P. Yalamanchi, M. Sinha, C. Dall'Osso, D. Khong, J. L. Shadrach, C. M. Miller, B. S. Singer, A. Stewart, N. Psychogios, R. E. Gerszten, A. J. Hartigan, M. J. Kim, T. Serwold, A. J. Wagers, R. T. Lee, *Cell* **2013**, *153*, 828.
- [2] T. Poggioli, A. Vujic, P. Yang, C. Macias-Trevino, A. Uygur, F. S. Loffredo, J. R. Pancoast, M. Cho, J. Goldstein, R. M. Tandias, E. Gonzalez, R. G. Walker, T. B. Thompson, A. J. Wagers, Y. W. Fong, R. T. Lee, *Circ. Res.* **2016**, *118*, 29.
- [3] R. G. Walker, T. Poggioli, L. Katsimpardi, S. M. Buchanan, J. Oh, S. Wattrus, B. Heidecker, Y. W. Fong, L. L. Rubin, P. Ganz, T. B. Thompson, A. J. Wagers, R. T. Lee, *Circ. Res.* **2016**, *118*, 1125.
- [4] a) E. J. Goebel, R. A. Corpina, C. S. Hinck, M. Czepnik, R. Castonguay, R. Grenha, A. Boisvert, G. Miklossy, P. T. Fullerton, M. M. Matzuk, V. J. Idone, A. N. Economides, R. Kumar, A. P. Hinck, T. B. Thompson, *Proc. Natl. Acad. Sci. U. S. A.* **2019**, *116*, 15505; b) R. G. Walker, M. Czepnik, E. J. Goebel, J. C. McCoy, A. Vujic, M. Cho, J. Oh, S. Aykul, K. L. Walton, G. Schang, D. J. Bernard, A. P. Hinck, C. A. Harrison, E. Martinez-Hackert, A. J. Wagers, R. T. Lee, T. B. Thompson, *BMC Biol* **2017**, *15*, 19.
- [5] M. A. Egerman, S. M. Cadena, J. A. Gilbert, A. Meyer, H. N. Nelson, S. E. Swalley, C. Mallozzi, C. Jacobi, L. L. Jennings, I. Clay, G. Laurent, S. Ma, S. Brachat, E. Lach-Trifilieff, T. Shavlakadze, A. U. Trendelenburg, A. S. Brack, D. J. Glass, *Cell Metab.* **2015**, *22*, 164.
- [6] M. J. Schafer, E. J. Atkinson, P. M. Vanderboom, B. Kotajarvi, T. A. White, M. M. Moore, C. J. Bruce, K. L. Greason, R. M. Suri, S. Khosla, J. D. Miller, H. R. Bergen 3rd, N. K. LeBrasseur, *Cell Metab.* **2016**, *23*, 1207.
- [7] R. D. Semba, P. Zhang, M. Zhu, E. Fabbri, M. Gonzalez-Freire, O. D. Carlson, R. Moaddel, T. Tanaka, J. M. Egan, L. Ferrucci, *J. Gerontol. A Biol. Sci. Med. Sci.* **2019**, *74*, 129.
- [8] B. MacLean, D. M. Tomazela, N. Shulman, M. Chambers, G. L. Finney, B. Frewen, R. Kern, D. L. Tabb, D. C. Liebler, M. J. MacCoss, *Bioinformatics* **2010**, *26*, 966.
- [9] C. D. L. Nguyen, S. Malchow, S. Reich, S. Steltgens, K. V. Shuvaev, S. Loroch, C. Lorenz, A. Sickmann, C. B. Knobbe-Thomsen, B. Tews, J. Medenbach, R. Ahrends, *Sci. Rep.* **2019**, *9*, 8836.
- [10] J. Palandra, A. Quazi, L. Fitz, H. Rong, C. Morris, H. Neubert, *Proteomics - Clin. Appl.* **2016**, *10*, 597.
- [11] U. H. Toprak, L. C. Gillet, A. Maiolica, P. Navarro, A. Leitner, R. Aebbersold, *Mol. Cell. Proteomics* **2014**, *13*, 2056.
- [12] a) V. Sharma, J. Eckels, B. Schilling, C. Ludwig, J. D. Jaffe, M. J. MacCoss, B. MacLean, *Mol. Cell. Proteomics* **2018**, *17*, 1239; b) J. A. Vizcaino, E. W. Deutsch, R. Wang, A. Csordas, F. Reisinger, D. Rios, J. A. Dianes, Z. Sun, T. Farrah, N. Bandeira, P. A. Binz, I. Xenarios, M. Eisenacher, G. Mayer, L. Gatto, A. Campos, R. J. Chalkley, H. J. Kraus, J. P. Albar, S. Martinez-Bartolome, R. Apweiler, G. S. Omenn, L. Martens, A. R. Jones, H. Hermjakob, *Nat. Biotechnol.* **2014**, *32*, 223.